科技部補助

大專學生研究計畫研究成果報告

計畫名稱：	Role of PIEZO2 channel gene knockdown in mast cells in cisplatin-induced mechanical hypersensitivity

報告類別：成果報告
執行計畫學生：洪俐
學生計畫編號：MOST 110-2813-C-040-019-B
研究期間：110年07月01日至111年02月28日止，計8個月
指導教授：曾拓榮

處理方式：本計畫可公開查詢

執行單位：中山醫學大學醫學系解剖學科

中華民國　111年03月24日

目錄

摘要

Chemotherapy-induced peripheral neuropathy (CIPN) and its associated neuropathic pain are one of the challenging complications in cancer treatment clinically. Platinum (Pt)-based analogues, a main class of chemotherapeutic agents, can cause neurotoxicity and extensively modulate the immune system. Our proposal is ongoing investigation regarding whether the interaction between cutaneous nerve fibers and mast cells (MCs) potentiates a critical molecular cross-talk and, indeed, participates in the initiation of mechanical hypersensitivity during treatment with cisplatin.

Here, we hypothesize the sequential mechanisms in cisplatin-induced mechanical hypersensitivity, including: (1) degeneration of subepidermal nerve fibers (SENFs) promotes the release of neuropeptides (calcitonin gene-related peptide (CGRP)); (2) neurogenic inflammation is therefore induced by CGRP, leading to MCs accumulation; (3) MCs degranulation is modulated through the PIEZO-type mechanosensitive ion channels/protein kinase C (PKC) signaling; and then (4) released pro-inflammatory cytokines and the potential receptors are involved in the process of mechanical hypersensitivity.

About the possible mechanisms of peripheral sensitization in rats with cisplatin treatment, our preliminary results indicate that (1) mechanical hypersensitivity, such as mechanical allodynia and mechanical hyperalgesia, was induced; (2) significant degeneration of SENFs was demonstrated by partial loss of SENFs and downregulated CGRP –immunoreactivity (ir) expressions in SENFs; (3) MCs accumulation was observed by the increases of chymase-ir expressions in MCs, which were parallel to those of PIEZO2 ion channel-ir expressions; (4) phosphorylated PKC (pPKCα, pPKCβII, pPKCγ)-ir expressions were not stained in MCs in the corresponding area ; (5) importantly, toll-like receptors (TLR4, TLR5 and TLR7) and chemokine C-X-C motif receptors (CXCR4 and CXCR7) were not expressed expectedly in SENFs; and (6) transient receptor potential cation channels vanilloid subtype (TRPV1 and TRPV4)-ir expressions were also not observed in SENFs by the immunohistochemistry.

Even though we could not observe PKC activation, TLR, CXCR and TRPV expressions in SENFs precisely, we detected intense increases of PIEZO2 ion channel in MCs, which means that PIEZO2 ion channel might play a main role in signaling the cisplatin-induced neuropathic pain. Thus, we can target PIEZO2 ion channel on the exploration of neurogenic inflammation and investigate the potential mechanisms of cisplatin-induced peripheral sensitization. Currently, much of our morphological evidence in the skin points to strong associations rather than specific mechanisms of action, which also implicate MCs-dependent mechanical hypersensitivity where MCs-targeted therapies may be most effective and beneficial in cisplatin-induced CIPN.

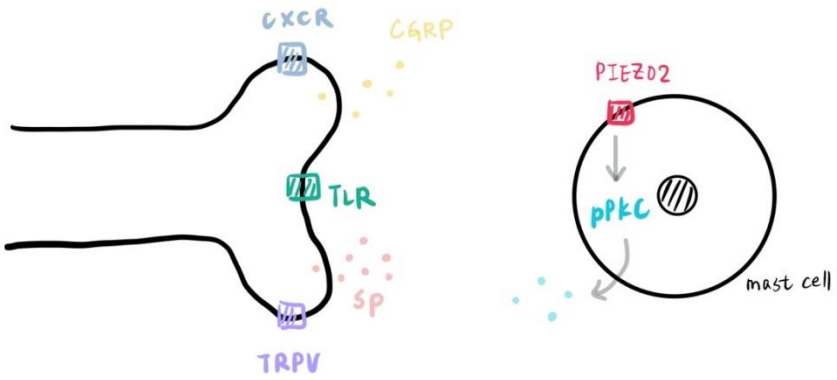

Keywords: cisplatin, mechanical hypersensitivity, PIEZO2 ion channel, protein kinase C, toll-like receptors, chemokine C-X-C motif receptors, transient receptor potential cation channels vanilloid subtype

前言

Chemotherapy-induced peripheral neuropathy (CIPN) and its associated neuropathic pain are one of the challenging complications in cancer treatment clinically.

研究目的

To verify whether the cisplatin-induced cutaneous nerve degeneration initiates the neurogenic inflammation, which leads to MCs activate PIEZO-type mechanosensitive ion channels/ PKC signaling for degranulation that modulates the receptors-involved mechanical hypersensitivity.

We propose experiments in rats injected with cisplatin to extend these observations by

1) determining whether cisplatin can affect the integrity of cutaneous SENFs innervation,

2) determining whether cisplatin induce the reduction of peptidergic SENFs,

3) determining whether the potential receptors, PIEZO-type mechanosensitive ion channels (PIEZO1 and PIEZO2 ion channels), can be up-regulated for modulating MCs degranulation,

4) determining whether the PKC signaling, such as PKCα, PKCβII and PKCr, can be activated in MCs,

5) determining whether the potential receptors, TLR, CXCR, and TRPV, are associated with cisplatin -induced mechanical hypersensitivity.

文獻探討

Famous chemotherapeutic agents include platinum (Pt)-based analogues, vinca alkaloids, taxanes derivatives, epothilones, thalidomide and bortezomib (Addington and Freimer, 2016; Boyette-Davis et al., 2015). The first agent of Pt-based analogues is cisplatin, *cis*-diamminedichloro-platinum, which acts by interstrand cross-linking and inhibiting deoxyribonucleic acid (DNA) replication (Karabajakian et al., 2017). Cisplatin induce side effects affecting up to 70% of patients with cancer that brings up a dose-limiting usage depending on chemotherapy regimen, treatment duration, patient age and concomitant therapies (Avan et al., 2015). Symmetrical sensory abnormalities, containing numbness, tingling, hypersensitivity and spontaneous pain, are occurred in patients treated with cisplatin (Clark et al., 2013; Park, 2014). Therefore, these patients suffer from physical pain symptoms that negatively impacts quality-of-life and treatments, occasionally resulting in the dose reductions and/or premature discontinuation of chemotherapy (Avan et al., 2015).

Primary afferents from the dorsal root ganglion (DRG) neurons are classified into distinct fibers, which are known that unmyelinated C fibers are primarily nociceptors and myelinated Aδ fibers conduct as mechanonociceptors, whereas myelinated Aβ fibers convey the light touch from mechanical stimuli (Basbaum et al., 1991). Recently, several clinical studies about painful peripheral neuropathy have used the skin biopsies to focus on primary afferents in dermis that are described as subepidermal nerve fibers (SENFs) (Myers et al., 2013). Neuropeptides, such as calcitonin gene-related peptide (CGRP) and substance P, released from primary afferents, facilitate an increase in vasodilation and plasma extravasation, causing tissue edema (Gouin et al., 2017). Additionally, the degranulation of mast cells (MCs) induces the release of pro-inflammatory cytokines, i.e., tumor necrosis factor alpha (TNF-α), interleukin (IL) and interferon, mediate nerve terminal swelling and myelin extirpation like that detected in the early stages of Wallerian degeneration (Zhang et al., 2017; Wang and Lehky, 2012). These released inflammatory mediators initiate the infiltration of immune cells and contribute to the inflammatory response while also activating primary

afferents and causing further neuropeptide release (Gouin et al., 2017; Pinho-Ribeiro et al., 2017). Therefore, this progressive pathophysiologial process is in response to the release of neuropeptides from primary afferents in the skin, described as the neurogenic inflammation, suggesting a mechanistic association between cutaneous inflammation and neuropathic pain (Pinho-Ribeiro et al., 2017; Lin et al., 2008).

MCs play an essential role in both innate and adaptive immunity and a large body of literature demonstrates their possible functions through MCs degranulation (Gurish and Austen, 2012; Suto et al., 2006). Major inflammatory mediators, including the enzymes, biogenic amines, cytokines, neuropeptides and nerve growth factor (NGF), are released from the granules (Wernersson and Pejler, 2014). Importantly, MCs express a variety of activating receptors such as the IgG receptors, IgE receptor, complement receptors and toll-like receptors that mediate degranulation, eicosanoid generation and cytokine production (Marshall and Jawdat, 2004; Saitoh et al., 2003). PIEZO-type ion channels are dissimilar between Piezo1 and Piezo2 ion channels begins in vertebrates, where the two channels accomplish a number of mechanosensitive functions in various cells and tissues (Ikeda et al., 2014; Maksimovic et al., 2014; Woo et al., 2014). For example, Piezo2 ion channel is expressed in Merkel cells, outer hair cells, endothelial cells in the brain, enterochromaffin cells of the gut, and in the neurons of the somatosensory ganglia, where it plays a key role in mechanosensation and proprioception. However, the linkage of Piezo2 ion channel to the MCs has not been supported by the results in the models of peripheral neuropathy.

Compared to other ion channels, relatively little is known on the modulation of Piezo channels by intracellular signaling pathways. Intracellular second messengers, such as cyclic nucleotides and phospholipid-derived signaling molecules, regulate several ion channels. Phosphatidylinositol 4,5-bisphosphate [$PI(4,5)P_2$] is generated by two phosphorylation steps from phosphatidylinositol (PI) (Balla, 2013). PLC enzymes catalyze the hydrolysis of $PI(4,5)P_2$ and the formation of the two classical second messengers inositol 1,4,5-trisphosphate (IP_3) and diacylglycerol (DAG). IP_3 induces Ca^{2+} release from the endoplasmic reticulum, by binding to its receptor, which is a Ca^{2+} permeable ion channel. DAG is an activator of protein kinase C (PKC). Conventional PKC isoforms (PKCα, β1, β2 and γ) are activated by DAG and Ca^{2+}. Novel PKC isoforms (PKCδ, ε, θ, and η) are Ca^{2+} insensitive, but they are activated by DAG, and their affinity for this lipid is much higher than that of conventional isoforms (Newton, 2010).

研究方法

Animals

Adult male Sprague-Dawley rats weighing 250–300 g used in these experiments are placed in a temperature- and humidity-controlled room with a 12 h light/dark cycle. All the procedures are conducted in accordance with the ethical guidelines set up by the International Association for the Study of Pain (IASP) on the use of laboratory animals in the experimental research and the protocol is approved by the Animal Committee of Chung Shan Medical University College of Medicine, Taichung, Taiwan (IASP Committee, 1980; Zimmermann, 1983).

Procedures

To investigate the acute effects of cisplatin, we perform the rats following well-established procedures for inducing neurotoxicity, using an injection volume of 1 ml/kg by an i.p. injection. All the rats are divided into three groups: (1) high dose of cisplatin: The group of rats (n = 15) are injected with cisplatin (10 mg/kg, Tocris Bioscience, Ellisville, MS); (2) low dose of cisplatin: The group of rats (n = 15) are injected

withcisplatin (1 mg/kg, Tocris Bioscience, Ellisville, MS); and (3) control (n = 9) are injected with 0.9% saline solution (Sigma Chemicals)(Akman et al., 2015). All the rats in each group are divided after an i.p. injection for the assessments of mechanical hypersensitivity at the following time points (post-injection week (PIW) 1, PIW 2 and PIW 4 and sacrificed at the same time points.

Behavioral assessments

1. Mechanical allodynia

Innocuous stimulation is determined by measuring the withdrawal thresholds with a series of calibrated Von Frey filaments (Senselab aesthesiometer, Somedic Sales AB, Stockholm) according to an up-and-down method.

2. **Thermal hyperalgesia**

Thermal hyperalgesia is evaluated with a Hargreaves-type analgesiometer (Ugo Basile, Comerio-Varese, Italy).

Immunohistochemistry

At the end of all experiments, the rats are deeply anesthetized using pentobarbital (100 mg/kg, i.p.) and sacrificed by intracardiac perfusion of 4% paraformaldehyde in 0.1 M phosphate buffer (PB) at pH 7.4. After perfusion, the spinal cords are removed and further immersed in fixative for additional 6 h before shifted to 0.1 M PB for storage. Prior to sectioning, samples are rinsing thoroughly, cryoprotected with 30% sucrose in 0.1 M PB overnight ; then cut at a plane perpendicular to the epidermis in a thickness of 50 μm per section with a sliding microtome (HM440E; Microm, Walldorf), labeled sequentially, and stored at -20°C. The sections for immunohistochemistry are treated with 0.5% Triton X-100 in 0.5 M Tris buffer (Tris) at pH 7.6 for 30 min and processed for immunostaining. Briefly, the sections are quenched with 1% H_2O_2 in methanol, blocked with 5% normal goat serum in 0.5% nonfat dry milk/Tris, then incubated with primary antiserum including: (1) rabbit peripherin (1:1000, Millipore); (2) rabbit neurofilament 200 kD (NF200)(1:1000, Sigma); (3) mouse CGRP (1:100, Santa Cruz Biotechnology); (4) rabbit Chymase (1:1000, Epitomics); (5) rabbit PIEZO2 ion channel (1:200, Sigma Chemicals); (6) rabbit phospho-PKCα (pPKCα, 1:1000, Cell singnaling); (7) rabbit phospho-PKCβII (pPKCβII, 1:1000, Cell singnaling); (8) rabbit phospho-PKCγ (pPKCγ, 1:1000, Epitomics); (9) rabbit TLR4 (1:200, proteintech); (10) rabbit TLR5 (1:200, proteintech); (11) rabbit TLR7 (1:200, proteintech); (12) rabbit CXCR4 (1:200, proteintech); (13) rabbit CXCR7 (1:200, proteintech); (9) rabbit TRPV1 (1:200, Millipore); and (15) rabbit TRPV4 (1:200, proteintech) at 4 °C overnight. After rinsing in Tris, the sections are incubated with biotinylated goat anti-rabbit IgG and anti-mouse IgG (1:100; Jackson ImmunoResearch Laboratories) for 1 h followed by avidin-biotin complex horseradish peroxidase reagent (Vector Laboratories) for another hour and the reaction products are demonstrated with 3,3'-diaminobenzidine (DAB, Sigma–Aldrich Co.).

Imaging analysis

A. SENFs areas

The standard procedure for measuring ir SENFs area is carried out according to a protocol published in our previous study (Ko et al., 2016).

B. Immune cells

Standard procedure is following a protocol modified from a published method previously. Briefly, we first photographed the high-definition monochrome images under an Olympus microscope (BH2; Olympus) with

a digital camera at a magnification of 100×. All the ir cells in dermis are calculated with the Image Pro-Plus software (Media Cybernetics) and plotted as the histogram of the immune cell diameter.

Statistical analysis

The examiners are blinded to the grouping information when performing the procedures of measurement and quantification. Data following the Gaussian distribution are expressed as mean ± standard derivation of the mean and analyzed with parametric tests. Data not following the Gaussian distribution are analyzed with the nonparametric Mann–Whitney test. Data are analyzed by GraphPad Prism (GraphPad, San Diego, CA). $p< 0.05$ is considered statistically significant. Data from experiments are also performed by one-way repeated measures ANOVA with the post hoc Tukey–Kramer multiple comparison test between three or more independent groups.

結果與討論

當前，癌症是全世界死亡率的主要原因。由於醫學和現代技術的進步，靈敏的測試和診斷方法的出現為檢測提供了可能早期癌症以及使用包括化療藥物在內的日益有效的治療方法，使癌症倖存者的數量在上升：預計到 2022 年將增加 35%，從 2012 年的 1370 萬增加到 1800 萬。儘管這些倖存者可能已經戰勝了癌症，但由於許多綜合症導致癌症治療（包括疼痛）降低了生活質量，其中許多綜合症在完成癌症治療後常常會經歷很長的時間。用於癌症化學療法的藥物是阻止癌症進展的極其有效的工具，因為它們具有旨在消除快速分裂的癌細胞的眾多靶標和作用機制。不幸的是，這些藥物也會影響人體的正常細胞和結構，引起各種有害的，有時甚至是毀滅性的副作用（例如貧血，腹瀉，噁心，嘔吐，感染，神經系統變化，疲勞，脫髮，不育，疼痛和周邊神經病變），這可能需要縮減化療方案甚至停止化療，從而限制了癌症治療的有效性。

化學治療劑可破壞神經系統結構，並取決於個別化合物，可引起多種神經病變：大，小纖維，感覺和/或運動，脫髓鞘和軸突，顱和自主神經。在不同種類的藥物中，化學療法對神經系統的影響各不相同，具體取決於所用藥物的具體物理和化學性質及其單一或累積劑量。由抗腫瘤藥引起的最常見的神經病之一是被稱為化療引起的周邊神經病變（CIPN）的疾病。對周圍神經系統產生神經毒性作用的化學治療藥被用作針對最常見類型癌症的標準常規藥物。六種主要藥物導致周圍的感覺，運動和自主神經元受損，從而導致 CIPN 的發展：鉑類抗腫瘤藥（特別是奧沙利鉑和順鉑），長春花生物鹼（特別是長春新鹼和長春鹼），埃博黴素（依沙貝比隆），紫杉烷類（紫杉醇，多西他賽），蛋白酶體抑製劑（硼替佐米）和免疫調節藥物（沙利度胺）。其中，最具神經毒性的抗癌藥物是鉑類藥物，紫杉烷類藥物，依沙貝比隆和沙利度胺及其類似物。其他具有較低神經毒性但也常用的藥物是硼替佐米和長春花生物鹼。

CIPN 的患病率取決於藥物，報導的比率從 19%到超過 85%不等，在鉑類藥物（70-100%），紫杉烷類藥物（11-87%）中最高，沙利度胺及其類似物（20-60%）和依沙貝比隆（60-65%）。高劑量服用或累積暴露後可能會發生毒性。觀察到的症狀強度和持續時間各不相同，範圍從急性，短暫的熱感覺到周圍神經的永久性變化，伴有慢性疼痛和不可逆的神經損傷。臨床上，CIPN 表現為強度不同的感覺，運動和/或自主神經功能障礙。感官症狀通常首先出現，通常表現為典型的“手套和襪套”神經病變，四肢的最遠端出現最大的缺陷。症狀包括麻木，刺痛，觸摸感改變，振動減弱，觸摸和溫暖或涼爽的溫度引起的感覺異常和感覺異常。而且，疼痛的感覺包括自發性灼傷，射擊或電擊樣疼痛。以及機械性或熱性異常性疼痛或痛覺過敏經常發生。在嚴重的情況下，這些症狀可能會導致感覺知覺喪失。

許多臨床醫生認為 CIPN 是挽救生命或至少延長生命的療法，雖然其副作用對患者未來命運的具

有積極影響。然而，許多患者主要是從極度不愉快的抱怨的角度來判斷它，這會造成痛苦並因此大大降低其間的生活質量。考慮到化學療法誘發的生化和細胞變化的潛在慢性，參與化學療法的腫瘤學家應了解問題的嚴重性和嚴重性，應了解導致 CIPN 風險增加的因素，並且應意識到癌症倖存者可能需要終生的醫學監測和治療藥物性健康問題和合併症的事實。這非常重要，尤其是在鉑基抗癌劑和紫杉烷類藥物中；使用這些藥物，CIPN 可能在化療完成後仍然可以持續數年。因此，為了製定有效的預防和治療策略，需要對 CIPN 的危險因素和潛在機制有更好的了解。

1. Effects of cisplatin on body weights and mechanical hypersensitivity

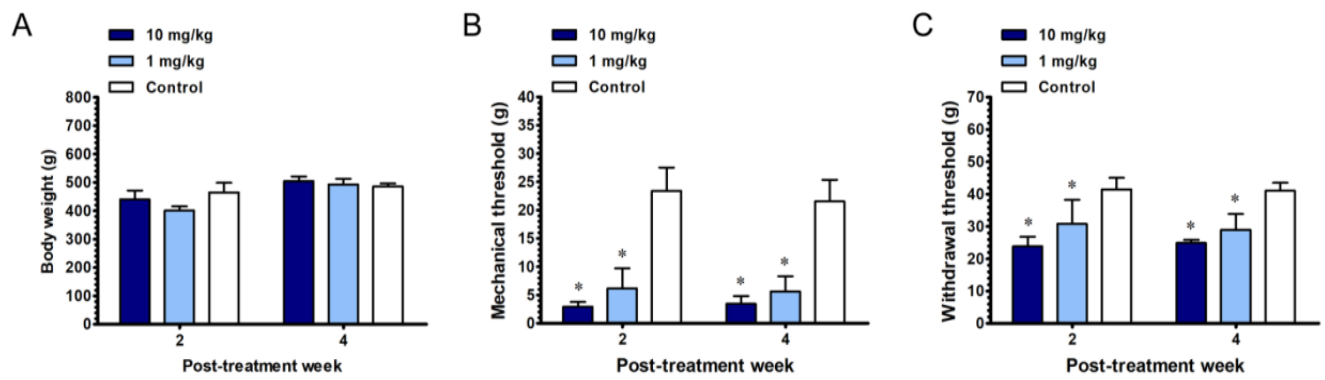

Fig. 1. Cisplatin-induced changes of body weights and mechanical hypersensitivity. The temporal changes of body weights were shown in (A) and possible changes of mechanical hypersensitivity were shown in (B) mechanical allodynia and (C) mechanical hyperalgesia. The degree of mechanical allodynia was represented as the mechanical threshold (g). The mechanical threshold of pinprick was demarcated as withdrawal threshold (g). All the measurements were expressed as the mean ± standard deviation (SD) at each post-injection week. Student's *t* test was applied to examine the differences against the values in the Control at each time point. * $p < 0.05$ indicated as a significant difference.

2. Influence of cisplatin in the distributions of SENFs in dermis.

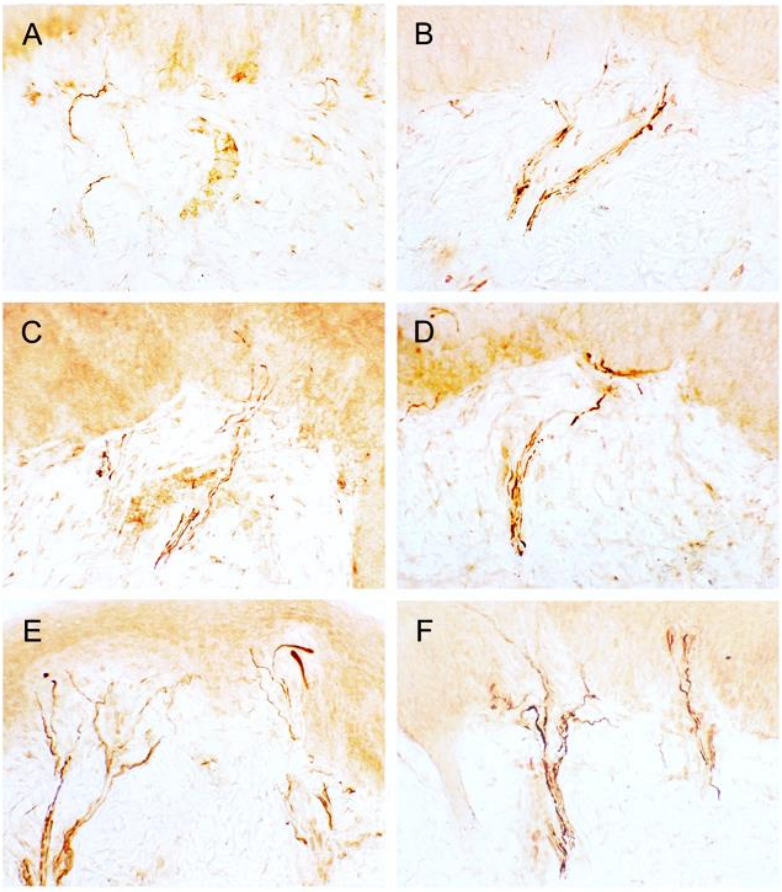

Fig. 2. Dermal changes of SENFs in the skin after cisplatin-induced peripheral neuropathy. The sections were immunostained with the antisera against (A, C, E) peripherin and (B, D, F) neurofilament 200kD (NF200). Graphs showed immunoreactive (ir) SENFs distributions in (A, B) the 10 mg/kg cisplatin group, (C, D) the 1 mg/kg cisplatin group, and (E, F) the Control group at post-injection week 2. Scale bar = 50 μm.

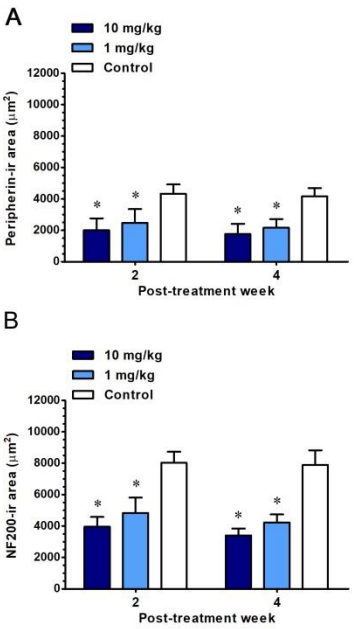

Fig. 3. Quantitation of cisplatin-induced SENFs degeneration in the skin. The changes of peripherin- and NF200-ir SENFs among the groups were expressed using a time-dependent manner. ∗, $p < 0.05$, indicate a significant difference.

3. Effects of cisplatin in the distributions of peptidergic SENFs in dermis.

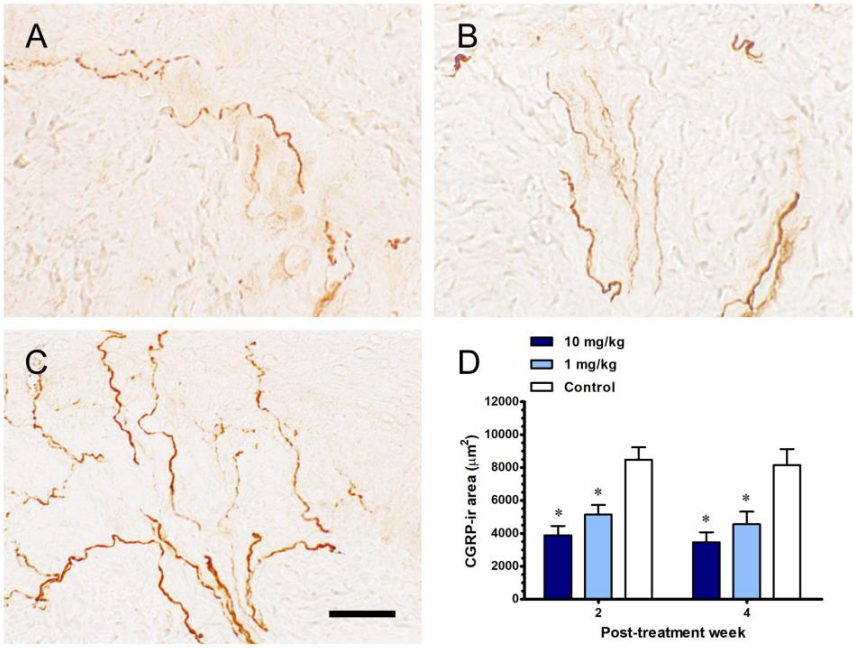

Fig. 4. Cisplatin-induced dermal changes of calcitonin gene-related peptide (CGRP)-immunoreactive (ir) expression in SENFs. The sections were immunostained with the antisera against calcitonin gene-related peptide (CGRP). Graphs showed **CGRP-ir** SENFs distributions in (A) the 10 mg/kg cisplatin group, (B) the 1 mg/kg cisplatin group, and (C) the Control group at post-injection week 4. Scale bar = 50 μm. (D) The changes of CGRP-ir SENFs among the groups were expressed using a time-dependent manner. ∗, $p< 0.05$, indicate a significant difference.

4. Influence of cisplatin in the dermal distribution of mast cells (MCs)

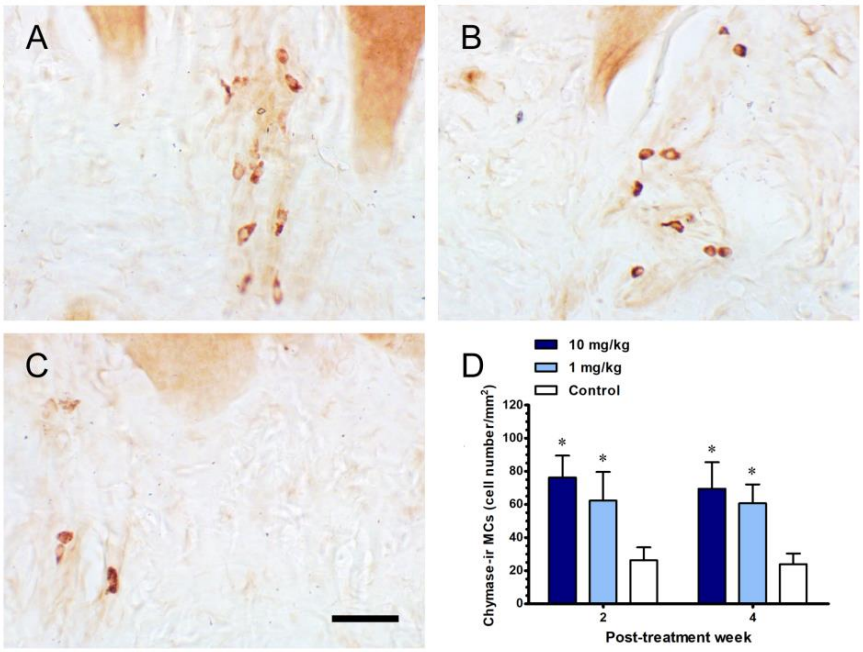

Fig.5. Distributions of mast cells (MCs) in dermis after cisplatin-induced peripheral neuropathy. The sections were immunostained with the antisera against chymase. Graphs showed chymase-ir MCs distributions in (A) the 10 mg/kg cisplatin group, (B) the 1 mg/kg cisplatin group, and (C) the Control group at post-injection week 4. Scale bar = 50 μm. (D) The changes of chymase-ir MCs among the groups were expressed time-dependently. ∗, $p< 0.05$, indicate a significant difference.

5. Effect of cisplatin on the expression of PIEZO2 ion channel in dermal MCs.

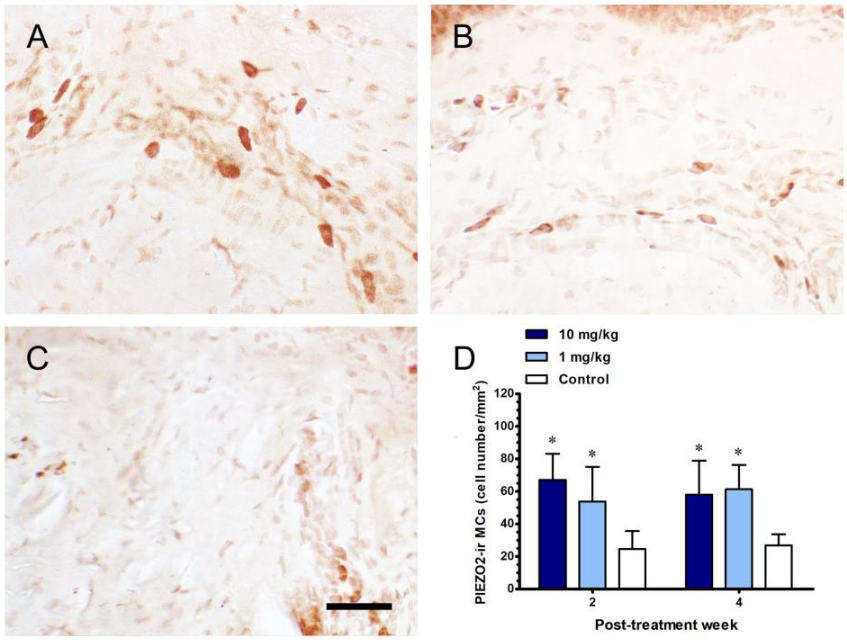

Fig. 6. Cisplatin leads to the activation of PIEZO2 channel in dermal MCs. The sections were immunostained with the antisera against PIEZO2 channel. Graphs showed PIEZO2 channel-ir MCs distributions in (A) the 10 mg/kg cisplatin group, (B) the 1 mg/kg cisplatin group, and (C) the Control group at post-injection week 4. Scale bar = 50 μm. (D) The changes of PIEZO2 channel-ir MCs among the groups were expressed in a time-dependent manner. ∗, $p < 0.05$, indicate a significant difference.

6. Possible downregulated protein kinases of PIEZO2 ion channel in MCs.

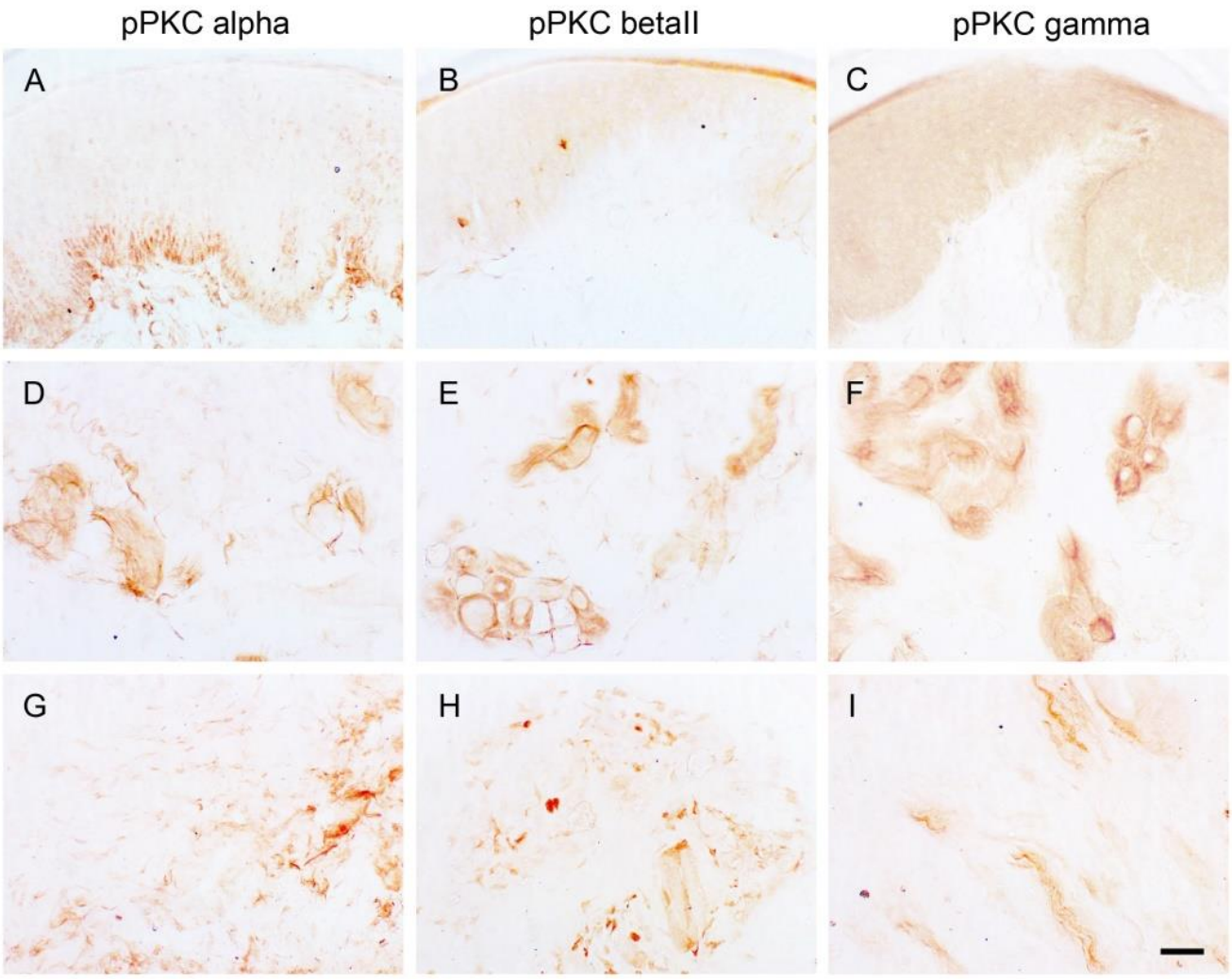

Fig. 7. Cisplatin induced the isoforms of protein kinase C (PKC) activation in dermis. The sections of 10 mg/kg cisplatin group were immunostained with the antisera against phosphorylated PKC (A, D, G: pPKCα, B, E, H: pPKCβII, C, F, I: pPKCγ). Graphs showed phosphorylated PKC distributions in (A, B, C) the superficial dermis, (D, E, F) the middle dermis, and (G, H, I) the deep dermis at post-injection week 4. Scale bar = 25 μm. Only the pPKCβII-ir expression was observed in MCs of the deep dermis.

7. Potential pain-related receptors l in SENFs or MCs.

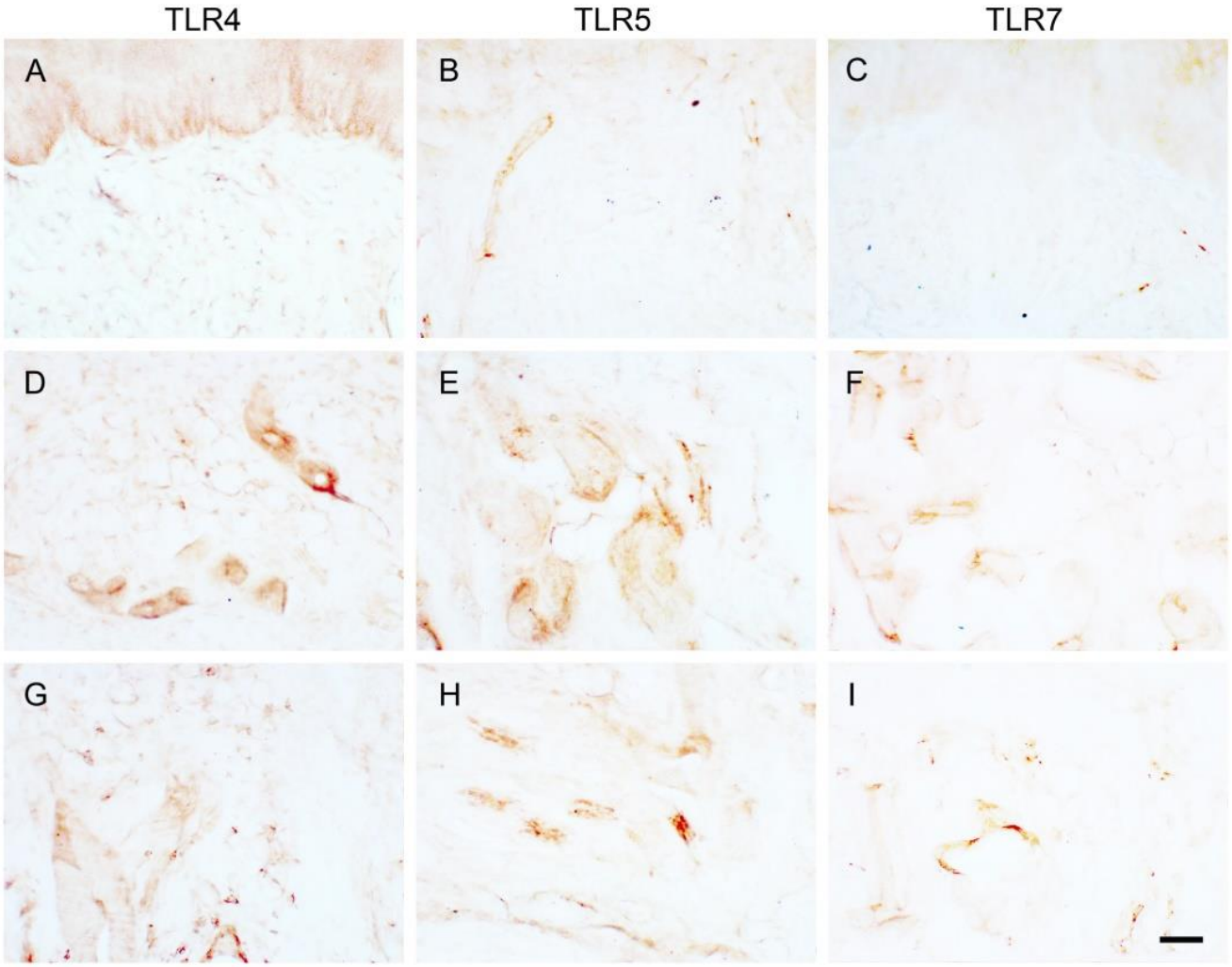

Fig. 8. Cisplatin induced the subtypes of toll-like receptors (TLR) distribution in dermis. The sections of 10 mg/kg cisplatin group were immunostained with the antisera against TLR4 (A, D, G), TLR5 (B, E, H), and TLR7 (C, F, I). Graphs showed subtypes of TLR distributions in (A, B, C) the superficial dermis, (D, E, F) the middle dermis, and (G, H, I) the deep dermis at post-injection week 4. Scale bar = 25 μm. Few TLR4-ir MCs and TLR5-ir nerve bundles were only observed in the deep dermis.

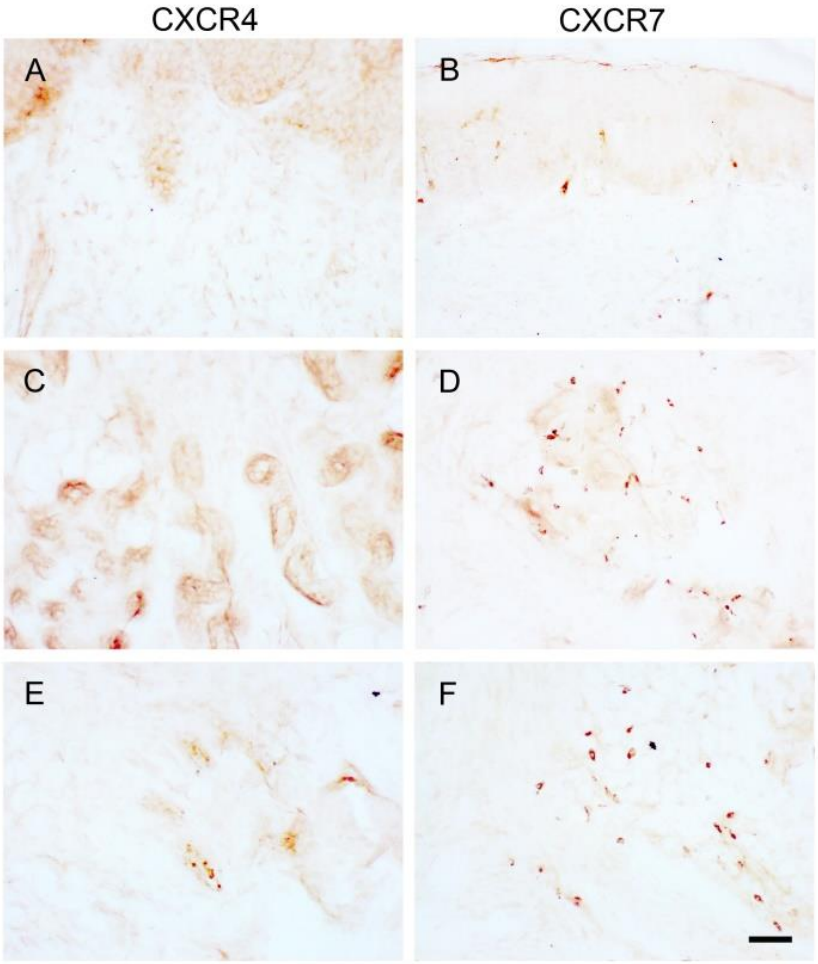

Fig. 9. Cisplatin induced the subtypes of chemokine C-X-C motif receptors (CXCR) distribution in dermis. The sections of 10 mg/kg cisplatin group were immunostained with the antisera against CXCR4 (A, C, E) and CXCR7 (B, D, F). Graphs showed subtypes of CXCR distributions in (A, B, C) the superficial dermis, (D, E, F) the middle dermis, and (G, H, I) the deep dermis at post-injection week 4. Scale bar = 25 μm. CXCR7-ir MCs were observed significantly in the middle and deep dermis.

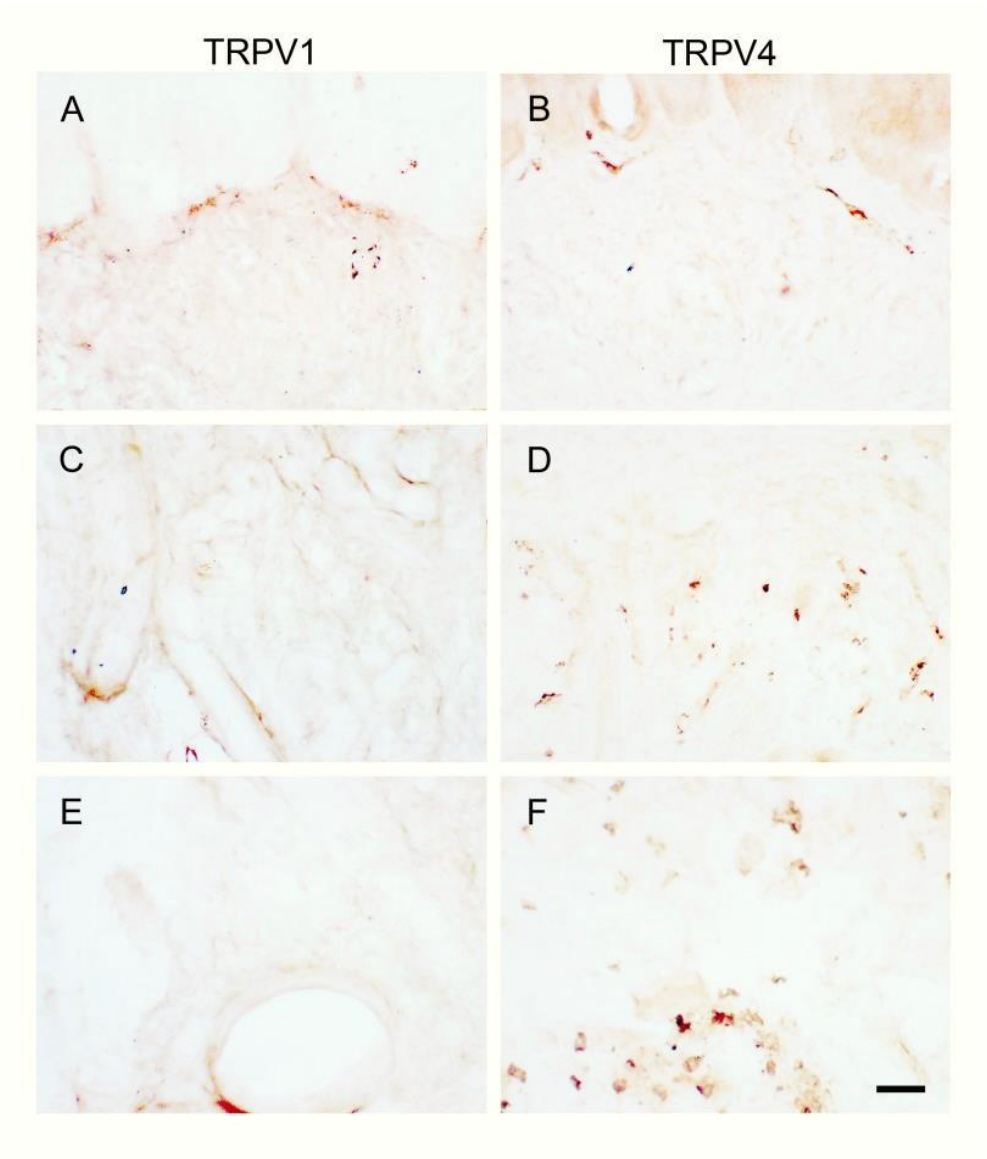

Fig. 10. Cisplatin induced the transient receptor potential cation channels vanilloid subtypes (TRPV) distribution in dermis. The sections of 10 mg/kg cisplatin group were immunostained with the antisera against TRPV1 (A, C, E) and TRPV4 (B, D, F). Graphs showed subtypes of TRPV distributions in (A, B, C) the superficial dermis, (D, E, F) the middle dermis, and (G, H, I) the deep dermis at post-injection week 4. Scale bar = 25 μm. TRPV4-ir MCs were observed significantly in the middle and deep dermis.

參考文獻

1. Addington J, Freimer M. Chemotherapy-induced peripheral neuropathy: an update on the current understanding Version 1. F1000Res. 2016;5: F1000 Faculty Rev-1466.
2. Boyette-Davis JA, Walters ET, Dougherty PM. Mechanisms involved in the development of chemotherapy-induced neuropathy. Pain Manag. 2015;5(4):285-296. Review.
3. Karabajakian A, Toussaint P, Neidhardt EM, Paulus V, Saintigny P, Fayette J. Chemotherapy for localized head and neck squamous cell cancers. Anticancer Drugs. 2017;28(4):362-368. Review.
4. Avan A, Postma TJ, Ceresa C, Avan A, Cavaletti G, Giovannetti E, Peters GJ. Platinum-induced neurotoxicity and preventive strategies: Past, present, and future. Oncologist. 2015;20(4):411-432.

5. Clark AK, Old EA, Malcangio M. Neuropathic pain and cytokines: Current perspectives. J Pain Res. 2013;6:803-814.
6. Park HJ. Chemotherapy induced peripheral neuropathic pain. Korean J Anesthesiol. 2014;67(1):4-7. Review.
7. Basbaum AI, Gautron M, Jazat F, Mayes M, Guilbaud G. The spectrum of fiber loss in a model of neuropathic pain in the rat: An electron microscopic study. Pain. 1991;47:359-367.
8. Myers MI, Peltier AC, Li J. Evaluating dermal myelinated nerve fibers in skin biopsy. Muscle Nerve. 2013;47:1-11.
9. Gouin O, L'Herondelle K, Lebonvallet N, Le Gall-Ianotto C, Sakka M, Buhé V, Plée-Gautier E, Carré JL, Lefeuvre L, Misery L, Le Garrec R. TRPV1 and TRPA1 in cutaneous neurogenic and chronic inflammation: pro-inflammatory response induced by their activation and their sensitization. Protein Cell. 2017;8(9):644-661.
10. Zhang X, Chen WW, Huang WJ. Chemotherapy-induced peripheral neuropathy. Biomed Rep. 2017;6(3):267-271.
11. Wang XM, Lehky TJ. Discovering cytokines as targets for chemotherapy-induced painful peripheral neuropathy. Cytokine. 2012;59(1):3-9.
12. Pinho-Ribeiro FA, Jr Verri WA, Chiu IM. Nociceptor sensory neuron-immune interactions in pain and inflammation. Trends Immunol. 2017;38(1):5-19.
13. Lin YY, Tseng TJ, Hsieh YL, Luo KR, Lin WM, Chiang H, Hsieh ST. Depletion of peptidergic innervation in the gastric mucosa of streptozotocin-induced diabetic rats. Exp Neurol. 2008;213(2):388-396.
14. Gurish MF, Austen KF. Developmental origin and functional specialization of mast cell subsets. Immunity. 2012;37(1):25-33.
15. Suto H, Nakae S, Kakurai M, Sedgwick JD, Tsai M, Galli SJ. Mast cell-associated TNF promotes dendritic cell migration. J Immunol. 2006;176(7):4102-4112.
16. Wernersson S, Pejler G. Mast cell secretory granules: armed for battle. Nat Rev Immunol. 2014;14(7):478-494.
17. Marshall JS, Jawdat DM. Mast cells in innate immunity. J Allergy Clin Immunol. 2004;114(1):21-27.
18. Saitoh S, Odom S, Gomez G, Sommers CL, Young HA, Rivera J, Samelson LE. The four distal tyrosines are required for LAT-dependent signaling in FcepsilonRI-mediated mast cell activation. J Exp Med. 2003;198(5):831-843.
19. Ikeda R, Cha M, Ling J, Jia Z, Coyle D, Gu JG. Merkel cells transduce andencode tactile stimuli to drive abeta-afferent impulses. Cell. 2014;157:664e675.
20. Maksimovic S, Nakatani M, Baba Y, Nelson AM, Marshall KL, Wellnitz SA, Firozi P, Woo SH, Ranade S, Patapoutian A, Lumpkin EA. Epidermal Merkel cells are mechanosensory cells that tune mammalian touch receptors.Nature. 2014;509(7502):617-621.
21. Woo SH, Ranade S, Weyer AD, Dubin AE, Baba Y, Qiu Z, Petrus M, Miyamoto T, Reddy K, Lumpkin EA, Stucky CL, Patapoutian A. Piezo2 is required for Merkel-cellmechanotransduction.Nature. 2014;509(7502):622-626.
22. Balla T. Phosphoinositides: tiny lipids with giant impact on cell regulation. Physiol Rev. 2013;93:

1019-1137.
23. Newton AC. Protein kinase C: poised to signal. Am J Physiol Endocrinol Metab. 2010;298:E395–402.
24. IASP Committee. Ethical standards for investigations of experimental pain in animals. The Committee for Research and Ethical Issues of the International Association for the Study of Pain. Pain. 1980;9:141-143.
25. Akman T, Akman L, Erbas O, Terek MC, Taskiran D, Ozsaran A. The preventive effect of oxytocin to Cisplatin-induced neurotoxicity: an experimental rat model. Biomed Res Int. 2015;2015:167235.
26. Ko MH, Yang ML, Youn SC, Lan CT, Tseng TJ. Intact subepidermal nerve fibers mediate mechanical hypersensitivity via the activation of protein kinase C gamma in spared nerve injury. Mol Pain. 2016;12:1-15.
27. Samur DN, Arslan R, Aydın S, Bektas N. Valnoctamide: The effect on relieving of neuropathic pain and possible mechanisms. Eur J Pharmacol. 2018;827:208-214.
28. Ko MH, Hsieh YL, Hsieh ST, Tseng TJ. Nerve demyelination increases metabotropic glutamate receptor subtype 5 expression in peripheral painful mononeuropathy. Int J Mol Sci. 2015;16(3):4642-4665.